INSTITUTE OF PHYSICS PUBLISHING NANOTECHNOLOGY
Nanotechnology **17** (2006) 3984–3988 doi:10.1088/0957-4484/17/15/063

Low-temperature, template-free synthesis of wurtzite ZnS nanostructures with hierarchical architectures

Huijuan Zhang and Limin Qi[1]

Beijing National Laboratory for Molecular Sciences, State Key Laboratory for Structural Chemistry of Unstable and Stable Species, College of Chemistry, Peking University, Beijing 100871, People's Republic of China

E-mail: liminqi@pku.edu.cn

Received 20 April 2006, in final form 28 June 2006
Published 11 July 2006
Online at stacks.iop.org/Nano/17/3984

Abstract
Hierarchical wurtzite ZnS architectures assembled from nanosheets and nanorods, such as branched flowers and fluffy solid and hollow spheres, have been synthesized by a facile, template-free, low-temperature solution route. The growth of wurtzite ZnS nanostructures at temperatures as low as 4 °C without any organic additives has been realized by the slow reaction between $Zn(NH_3)_4^{2+}$ and thioacetamide in aqueous $(NH_4)_2SO_4$–NH_4OH solutions. Branched ZnS flowers made of ultrathin nanosheets ∼6–10 nm in thickness were produced at 4 °C, whereas fluffy ZnS spheres consisting of radially oriented nanorods were fabricated at 60 °C. Prolonged ageing of the fluffy spheres at 60 °C resulted in the formation of unique fluffy hollow ZnS spheres through a spontaneous hollowing process based on Ostwald ripening.

1. Introduction

As an important semiconductor with a wide band-gap energy (3.6 eV), ZnS has attracted considerable attention due to its applications in flat-panel displays, electroluminescence devices, photonic crystal devices, sensors, lasers, and photocatalysis [1–3]. Many recent efforts have been devoted to the controlled synthesis of ZnS nanostructures with various forms including nanoparticles [3], nanorods [4], nanobelts [5, 6], nanotubes [7], nanosheets [8], aligned tetrapods [9], nanowire bundles [10, 11], and hollow spheres [12–16]. It is known that ZnS adopts two structural polymorphs, i.e. hexagonal wurtzite and cubic sphalerite (zinc blende), with the wurtzite phase being the high-temperature polymorph of sphalerite. Considering that wurtzite ZnS is much more desirable for its optical properties than the sphalerite phase, the low-temperature synthesis and stabilization of wurtzite ZnS nanostructures is extremely practical [1, 2]. Notably, wurtzite ZnS nanocrystals were fabricated in a polyol medium at temperatures as low as 150 °C [17]. Subsequently, the hydrothermal synthesis of wurtzite ZnS hollow spheres at 140 °C was reported [14]. However, scientists have just begun to explore the room-temperature synthesis of wurtzite ZnS nanostructures. In this regard, biological templates have been successfully used to control the crystal phase of ZnS nanocrystals at room temperature. For example, peptide sequences identified by phage display libraries were employed to direct the specific nucleation and growth of either the wurtzite or sphalerite ZnS nanocrystals [18, 19]. Recently, wurtzite ZnS nanocrystals were grown on Zn finger-like peptide nanotubes at room temperature, where the peptide template approach and the nucleation-site controlling approach were combined to control the ZnS crystal phase [2]. Nevertheless, it remains a great challenge to explore low-temperature, template-free routes to wurtzite ZnS nanostructures.

In recent years, the self-assembly and higher-order organization of nanostructured building blocks into complex architectures has been of intense interest in current materials synthesis and nanodevice fabrication [20–26]. Hence it is worthwhile exploring the low-temperature fabrication of wurtzite ZnS nanostructues with hierarchical architectures self-assembled from one- and two-dimensional (1D, 2D) nanoscale building blocks. It is noted that considerable effort has been devoted to the controlled synthesis of hollow ZnS spheres [12–16]; however, reports on the self-assembly of 1D

[1] Author to whom any correspondence should be addressed.

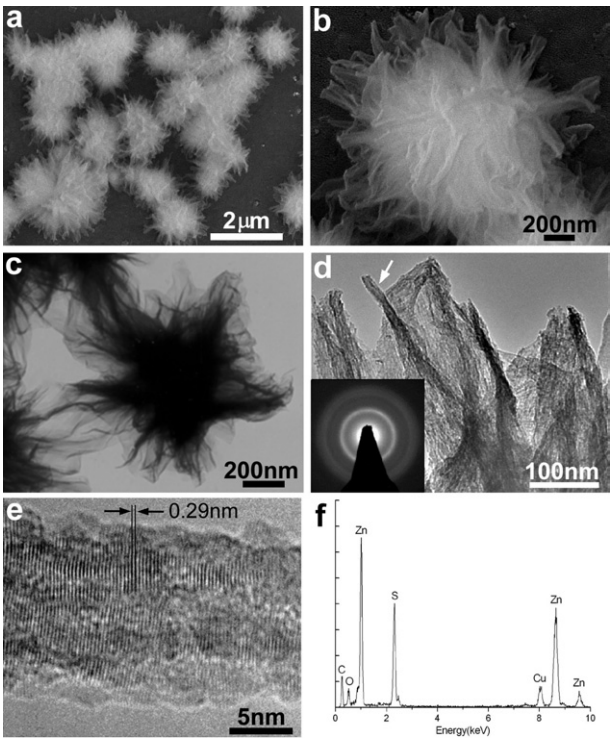

Figure 1. SEM ((a), (b)), TEM ((c), (d)) and HRTEM (e) images and EDS spectrum (f) of branched ZnS flowers obtained at 4 °C. The inset shows the related ED pattern. The HRTEM image shown in (e) is enlarged from the protrusion indicated by the arrow in (d). $[Zn(NH_3)_4^{2+}] = 5.5$ mM.

and 2D ZnS nanostructures into complex three-dimensional (3D) architectures are still rare. Herein, we report a facile, template-free synthesis of wurtzite ZnS nanostructures with hierarchical architectures, such as branched flowers and fluffy hollow spheres, in low-temperature (4–60 °C) aqueous solutions.

2. Experiments

2.1. Materials

Thioacetamide (CH_3CSNH_2), ZnO, $ZnSO_4$, $(NH_4)_2SO_4$, and NH_4OH were of analytical grade. All the chemicals were used as received and the water used was deionized.

2.2. Synthesis

Fabrication of wurtzite ZnS architectures was achieved simply by the slow reaction between $Zn(NH_3)_4^{2+}$ and thioacetamide (TAA) in aqueous $(NH_4)_2SO_4$–NH_4OH buffer solutions. In the typical synthesis of ZnS flowers and fluffy spheres, 1 mg of ZnO was dissolved in 1 ml of mixed solution of 1M $(NH_4)_2SO_4$ and 12 M NH_4OH, which was followed by the addition of 1.23 ml of 10 mM TAA solution, giving a final concentration of 5.5 mM for both $Zn(NH_3)_4^{2+}$ and TAA. The clear mixture was left to stand under static conditions at a given temperature (4–60 °C) for 8 h, leading to the gradual formation of ZnS precipitates, which were collected by centrifugation, washed with water, and dried in air. For the synthesis of ZnS

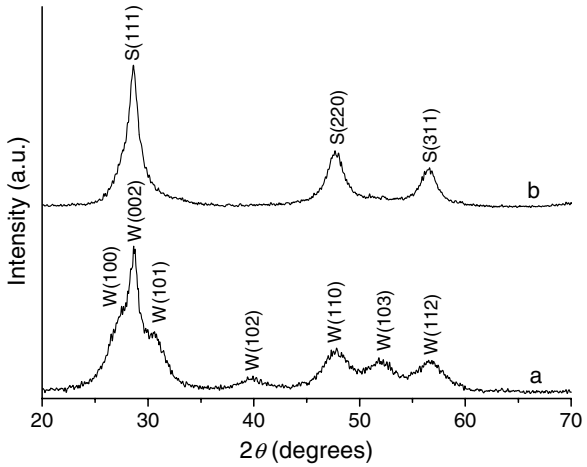

Figure 2. XRD patterns of ZnS products obtained at 4 °C with different reactant concentrations. $[Zn(NH_3)_4^{2+}]$: (a) 5.5 mM, (b) 550 mM. 'W' and 'S' before the indices denote the hexagonal wurtzite and cubic sphalerite ZnS, respectively.

fluffy hollow spheres, the reaction mixture was left to age at 60 °C for 3 days.

2.3. Characterization

The products obtained were characterized by scanning electron microscopy (SEM, FEI STRATA DB235, 10 kV), transmission electron microscopy (TEM, JEOL JEM 200CX, 160 kV), and high-resolution TEM (HRTEM, FEI TECNAI F30, 300 kV) together with associated energy-dispersive x-ray spectroscopy (EDS), powder x-ray diffraction (XRD, Rigaku Dmax-2000, Cu Kα), ultraviolet (UV)–visible spectroscopy (Shimadzu UV-250), and BET surface area measurements (Micromeritics ASAP 2010).

3. Results and discussion

The chemical precipitation of ZnS resulted from the reaction of the soluble zinc species, predominantly $Zn(NH_3)_4^{2+}$ at high NH_3 concentration [27], with the S^{2-} ions released from TAA, probably as follows:

$$Zn(NH_3)_4^{2+} + CH_3CSNH_2 + H_2O \rightarrow ZnS + CH_3CONH_2 + 2NH_3 + 2NH_4^+. \quad (1)$$

Figure 1(a) shows an overview SEM image of the flower-like ZnS product obtained after 8 h of ageing at 4 °C, which suggests that the highly branched flowers are about 1.0–2.3 μm in size. An enlarged SEM image (figure 1(b)) suggests that the flower is actually built from ultrathin, flexible ZnS nanosheets that emanated from the centre of the flower. The XRD pattern of these flowers (figure 2(a)) shows broadened diffraction peaks matching well with hexagonal ZnS of the wurtzite structure (JCPDS No. 80-0007), indicating the formation of wurtzite ZnS nanocrystallites. The XRD pattern of the ZnS flowers shows that the wurtzite (100), (002), and (101) peaks are strongly overlapping, which is in contrast to the three well-resolved peaks shown in the XRD pattern of the well-crystallized wurtzite ZnS nanobelts [1], indicating that the current wurtzite ZnS flowers could contain considerable

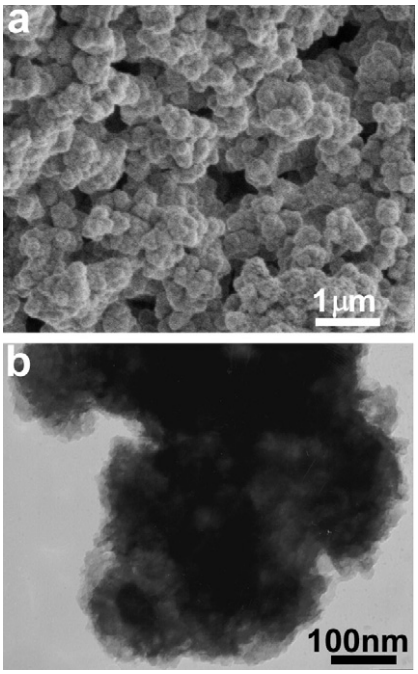

Figure 3. SEM (a) and TEM (b) of ZnS products obtained at 4 °C with a high reactant concentration; $[Zn(NH_3)_4^{2+}] = 550$ mM.

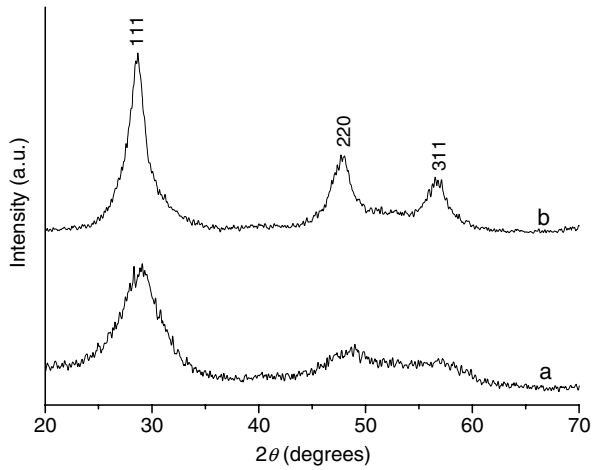

Figure 4. XRD patterns of sphalerite ZnS products obtained at 4 °C with different $(NH_4)_2SO_4$–NH_4OH concentrations:
(a) $[(NH_4)_2SO_4] = 0.45$ M, $[NH_4OH] = 1.1$ M;
(b) $[(NH_4)_2SO_4] = 0$, $[NH_4OH] = 5.4$ M.

structural disorder. A typical TEM image of a single ZnS flower (figure 1(c)) clearly shows the wrapped nanosheets, in good agreement with the SEM observation. A high-magnification TEM image (figure 1(d)) suggests that the nanosheets are so flexible that they can easily form folded structures (as indicated by the arrow) and the thickness of the nanosheets typically ranges from 6 to 10 nm. The related electron diffraction (ED) pattern shows relatively broad rings, in fairly good agreement with the (002), (102), (110), and (103) planes of wurtzite, indicating that the ZnS nanosheets are probably polycrystalline thin films consisting of wurtzite nanocrystallites. A representative HRTEM image enlarged from the folded protrusion is shown in figure 1(e), which exhibits clear, though somewhat irregular, lattice fringes with a spacing of 0.29 nm corresponding to the (101) plane of the wurtzite ZnS. The slight distortion of the lattices could be attributed to the irregular folding of the nanosheets. The chemical composition and the stoichiometry of the ZnS flowers were revealed by the EDS spectrum (figure 1(f)), which shows only the peaks for Zn and S, in addition to the Cu signal arising from the copper TEM grids and the normal C and O peaks. Elemental analysis reveals that the molar ratio of Zn/S is 50.4:49.6, in good agreement with the stoichiometric ZnS within experimental error (5–10%). The formation of the wurtzite ZnS phase at such a low temperature (4 °C) is quite surprising, since wurtzite ZnS nanocrystals are usually obtained at high temperature, typically higher than 140 °C [14], and until now the synthesis of wurtzite nanocrystals at temperatures as low as room temperature has been achieved only under the control of specific peptides [2]. The current low-temperature synthesis of branched ZnS flowers through the slow release of S^{2-} ions from TAA is reminiscent of the progressive growth of dendritic flowers built up of copper hydroxide nanosheets ∼40 nm in thickness under nearly sustained supersaturation [28]. To the best of our knowledge, this is the first low-temperature synthesis of such elaborate wurtzite ZnS flowers self-assembled from ultrathin nanosheets. The BET specific surface area of the ZnS flowers was measured to be as large as 220 ± 6 m^2 g^{-1}, much higher than that for the high-surface-area ZnS nanoporous nanoparticles (156 m^2 g^{-1}) obtained by the polyol route [3]. The current ZnS flowers with extremely high surface area may be considered as promising candidates for useful photocatalysts.

If the reactant concentration for both $Zn(NH_3)_4^{2+}$ and TAA was increased from the standard concentration (5.5 mM) to 550 mM under otherwise identical conditions, irregular aggregates were obtained (figure 3) and the corresponding XRD pattern (figure 2(b)) showed that the aggregates were actually pure sphalerite ZnS crystals. Moreover, it was revealed that an appropriate concentrated $(NH_4)_2SO_4$–NH_4OH buffer solution, e.g. a suitable free NH_3 concentration and a suitable pH, was essential for the low-temperature growth of the wurtzite ZnS crystals. For example, the synthesis conducted at the standard $(NH_4)_2SO_4$ concentration (0.45 M) but a lower NH_4OH concentration (1.1 M) and the synthesis conducted at the standard NH_4OH concentration (5.4 M) but without $(NH_4)_2SO_4$ just yielded pure sphalerite ZnS crystals (figure 4). These results demonstrate that the low-temperature synthesis of wurtzite ZnS nanostructures without organic templates can be realized only if suitable reaction conditions are selected to accurately control the nucleation and growth process of ZnS nanocrystals, e.g. a suitable free NH_3 concentration and pH for the controlled release of Zn^{2+} ions from $Zn(NH_3)_4^{2+}$ and S^{2-} ions from TAA, as well as an appropriate coordination environment for the ZnS crystal growth. This result indicates that, in the peptide-directed, room-temperature synthesis of wurtzite ZnS nanocrystals [2, 18], the biological templates containing functional groups may also provide a suitable chemical microenvironment to direct the specific nucleation and growth of wurtzite nanocrystals. However, the exact mechanism for the formation of pure wurtzite ZnS nanostructures at such a low temperature (4 °C) remains to be fully elucidated. It has been

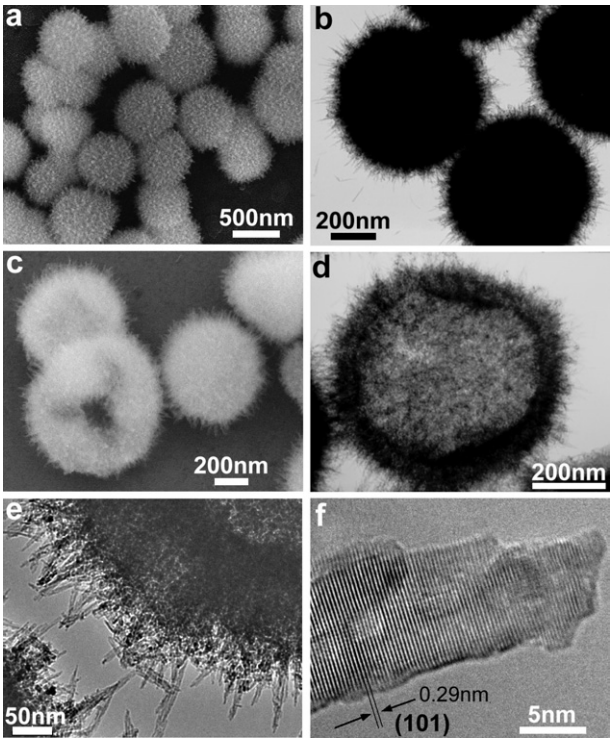

Figure 5. SEM ((a), (c)) and TEM ((b), (d)–(f)) images of fluffy ZnS spheres obtained after ageing at 60 °C for 8 h ((a), (b)) and 3 days ((c)–(f)).

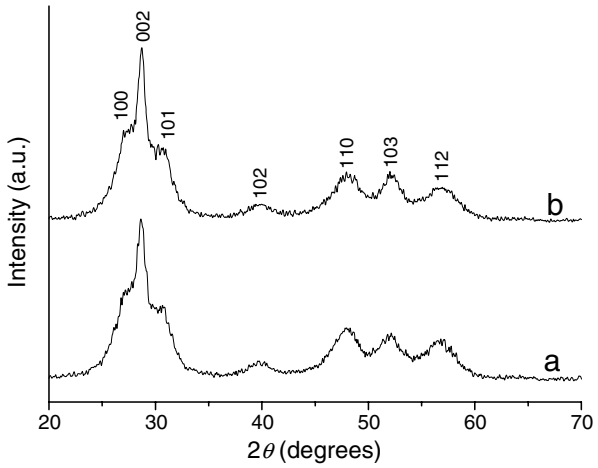

Figure 6. XRD patterns of fluffy wurtzite ZnS spheres obtained after ageing at 60 °C for 8 h (a) and 3 days (b).

documented that small wurtzite nanocrystals would be more thermodynamically stable than sphalerite nanocrystals because the transformation temperature of sphalerite to wurtzite decreases with decreasing ZnS particle size due to the effect of the surface energy [29]. In particular, the transformation temperature is dramatically lowered to about 25 °C for ZnS nanocrystals with an average size of ∼7 nm. Under the current synthesis conditions, the high free NH_3 concentration would provide a strong coordination environment, leading to the formation of primary ZnS nanoparticles mostly smaller than 7 nm, with the wurtzite phase being the thermodynamically stable phase at the low temperature (4 °C). Furthermore, it has been revealed that the phase stability of ZnS nanoparticles is also affected by the surface adsorption, and the stability of the wurzite phase may be decreased by the adsorbed water [29]. In the present situation, the presence of a high concentration of free NH_3 in the solution would considerably prevent the direct adsorption of water on the surface of ZnS nanoparticles, resulting in an enhanced stability of the wurtzite phase. Meanwhile, the slow release of Zn^{2+} ions from $Zn(NH_3)_4^{2+}$ and S^{2-} ions from TAA at a suitable free NH_3 concentration and pH would favour the nucleation and growth of thermodynamically stable wurtzite ZnS nanocrystals. As a consequence, small wurtzite nanocrystals would form initially and then self-assemble gradually into branched flowers consisting of ultrathin nanosheets ∼6–10 nm, which are stable in the concentrated $(NH_4)_2SO_4$–NH_4OH buffer solution.

When the reaction temperature was increased from 4 to 60 °C under the standard solution concentration conditions, the morphology of the ZnS products varied from highly branched flowers through relatively dense flowers to fluffy spheres, while the crystal phase remained as wurtzite ZnS. In particular, fluffy ZnS spheres about 600–800 nm in diameter, which consisted of a relatively dense core and a thin shell built from radially oriented nanorods, were obtained after ageing at 60 °C for 8 h (figures 5(a), (b)). Interestingly, the fluffy solid spheres evolved into fluffy hollow spheres with a wall thickness about 100 ± 20 nm after ageing at 60 °C for 3 days (figures 5(c), (d)). High-magnification TEM and HRTEM images suggests that the shell of the fluffy hollow spheres essentially consists of densely packed, outwardly extended wurtzite nanorods of about 8 ± 3 nm in diameter and that the nanorods have a preferential (101) growth plane (figures 5(e), (f)). The wurtzite ZnS structure of these fluffy solid and hollow spheres was confirmed by the related XRD patterns (figure 6). The measured BET surface areas of the fluffy solid and hollow spheres are ∼230 and ∼270 $m^2\ g^{-1}$, respectively, slightly larger than that for the branched ZnS flowers. Compared with the previously reported ZnS hollow spheres [12–16], the current fluffy hollow spheres are unique, in that they are hierarchical assemblies of ZnS nanorods.

The formation mechanism of the fluffy hollow spheres is still under investigation. However, our experimental results suggest that the fluffy hollow spheres evolved from the early fluffy solid spheres probably through a hollowing process based on Ostwald ripening [29]. As shown in figure 7, most of the fluffy spheres were still solid spheres after ageing at 60 °C for 1 day and a small portion of the fluffy spheres became hollow with a smaller empty core and a thicker shell after 2 days of ageing. After 3 days of ageing, most of the fluffy spheres developed into the fluffy hollow spheres with a similar outer diameter but a much thinner shell, as shown in figures 5(c) and (d). This result indicates that, initially, relatively loose cores were formed due to the relatively high reactant concentration at the beginning of the reaction. Then, the shell crystallites could grow gradually at the expense of the inner cores via Ostwald ripening, resulting in the formation of the final fluffy hollow spheres. Such a template-free route to inorganic hollow spheres based on Ostwald ripening has been used previously for the preparation of TiO_2 hollow spheres [30].

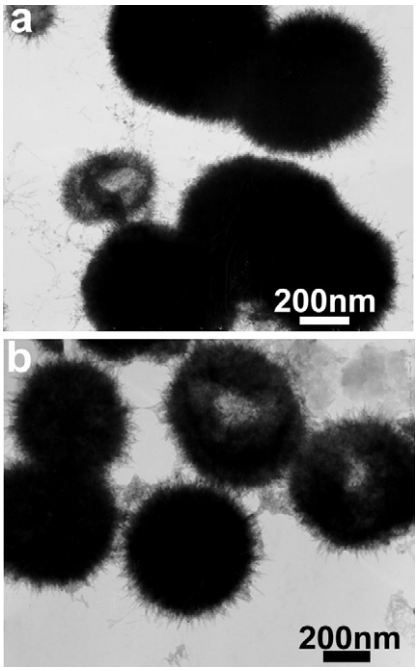

Figure 7. TEM images of fluffy ZnS spheres obtained after ageing at 60 °C for different times: (a) 1 d, (b) 2 d.

4. Conclusions

Novel wurtzite ZnS nanostructures with hierarchical architectures have been synthesized by a template-free solution route at low temperatures (4–60 °C). It has been demonstrated that the formation of wurtzite ZnS nanostructures at temperatures as low as 4 °C without any functional organic molecules can be realized in a suitable chemical environment. Branched ZnS flowers made of ultrathin nanosheets ∼6–10 nm in thickness were produced at 4 °C, whereas fluffy solid and hollow ZnS spheres consisting of radially oriented nanorods were fabricated at 60 °C. It was revealed that the fluffy hollow ZnS spheres evolved from the early fluffy solid spheres probably through a spontaneous hollowing process based on Ostwald ripening. The obtained hierarchical wurtzite ZnS architectures with extremely high surface area could find interesting applications in various fields including catalysis, sensing, and sorption. This facile synthetic strategy sheds new light on the biomineralization process, where elaborate inorganic architectures are produced in a natural environment [31], and it may be extendable to the low-temperature synthesis of complex architectures of other inorganic systems.

Acknowledgments

This work was supported by the National Natural Science Foundation of China (20325312, 20473003, 50521201, and 20233010) and the Foundation for the Author of National Excellent Doctoral Dissertation of China (200020).

References

[1] Wang Z, Daemen L L, Zhao Y, Zha C S, Downs R T, Wang X, Wang Z L and Hemley R J 2005 *Nat. Mater.* **4** 922
[2] Banerjee I A, Yu L and Matsui H 2005 *J. Am. Chem. Soc.* **127** 16002
[3] Hu J-S, Ren L-L, Guo Y-G, Liang H-P, Cao A-M, Wan L-J and Bai C-L 2005 *Angew. Chem. Int. Edn* **44** 1269
[4] Yu J H, Joo J, Park H M, Baik S-I, Kim Y W, Kim S C and Hyeon T 2005 *J. Am. Chem. Soc.* **127** 5662
[5] Ma C, Moore D, Li J and Wang Z L 2003 *Adv. Mater.* **15** 228
[6] Yao W-T, Yu S-H, Pan L, Li J, Wu Q-S, Zhang L and Jiang J 2005 *Small* **1** 320
[7] Yin L-W, Bando Y, Zhan J-H, Li M-S and Golberg D 2005 *Adv. Mater.* **17** 1972
[8] Yu S-H and Yoshimura M 2002 *Adv. Mater.* **14** 296
[9] Zhu Y-C, Bando Y, Xue D-F and Golberg D 2003 *J. Am. Chem. Soc.* **125** 16196
[10] Moore D F, Ding Y and Wang Z L 2004 *J. Am. Chem. Soc.* **126** 14372
[11] Zhu Y-C, Bando Y, Xue D-F and Golberg D 2004 *Adv. Mater.* **16** 831
[12] Ma Y, Qi L, Ma J and Cheng H 2003 *Langmuir* **19** 4040
[13] Zhang H, Zhang S, Pan S, Li G and Hou J 2004 *Nanotechnology* **15** 945
[14] Liu H, Ni Y, Han M, Liu Q, Xu Z, Hong J and Ma X 2005 *Nanotechnology* **16** 2908
[15] Wolosiuk A, Armagan O and Braun P V 2005 *J. Am. Chem. Soc.* **127** 16356
[16] Peng Q, Xu S, Zhuang Z, Wang X and Li Y 2005 *Small* **1** 216
[17] Zhao Y, Zhang Y, Zhu H, Hadjipanayis G C and Xiao J Q 2004 *J. Am. Chem. Soc.* **126** 6874
[18] Flynn C E, Mao C, Hayhurst A, Williams J L, Georgiou G, Iverson B and Belcher A M 2003 *J. Mater. Chem.* **13** 2414
[19] Mao C, Flynn C E, Hayhurst A, Sweeney R, Qi J, Georgiou G, Iverson B and Belcher A M 2003 *Proc. Natl Acad. Sci. USA* **100** 6946
[20] Whitesides G M and Grzybowski B 2002 *Science* **295** 2418
[21] Cölfen H and Mann S 2003 *Angew. Chem. Int. Edn* **42** 2350
[22] Cölfen H and Antonietti M 2005 *Angew. Chem. Int. Edn* **44** 5576
[23] Cao A-M, Hu J-S, Liang H-P and Wan L-J 2005 *Angew. Chem. Int. Edn* **44** 4391
[24] Liu B and Zeng H C 2004 *J. Am. Chem. Soc.* **126** 8124
[25] Shi H, Qi L, Ma J and Cheng H 2003 *J. Am. Chem. Soc.* **125** 3450
[26] Yang J, Qi L, Lu C, Ma J and Cheng H 2005 *Angew. Chem. Int. Edn* **44** 598
[27] Chaparro A M 2005 *Chem. Mater.* **17** 4118
[28] Zhang Z, Shao X, Yu H, Wang Y and Han M 2005 *Chem. Mater.* **17** 332
[29] Zhang H, Huang F, Gilbert B and Banfield J F 2003 *J. Phys. Chem.* B **107** 13051
[30] Yang H G and Zeng H C 2004 *J. Phys. Chem.* B **108** 3492
[31] Mann S 2001 *Biomineralization: Principles and Concepts in Bioinorganic Material Chemistry* (New York: Oxford University Press)